

Available at [www.jpbums.info](http://www.jpbums.info)

Original article

# Behavioral, Biochemical and Pathological Characterization of a new MDX Mouse Model of Duchenne Muscular Dystrophy

Fengjiao Wang<sup>1</sup>, Jing Wen<sup>1</sup>, Baojian Guo<sup>1</sup>, Liangmiao Wu<sup>1</sup>,  
Zheng Liu<sup>2,3</sup>, Zhang Zaijun<sup>1\*</sup>

## Author affiliations

<sup>1</sup>Institute of New Drug Research; International Cooperative Laboratory of Traditional Chinese Medicine Modernization and Innovative Drug Development of Chinese Ministry of Education, Jinan University College of Pharmacy, Guangzhou 510632, China

<sup>2</sup> School of Stomatology and Medicine & Foshan Stomatology Hospital, Foshan University, Foshan 528000, China

<sup>3</sup> Foshan Magpie Pharmaceuticals Co., LTD, Foshan, China

## Author contribution:

All authors contributed equally to this paper or author contribution: Wang, Fengjiao; Wen, Jing; Guo, Baojian; contributed towards data collection and analysis; Wu, Liangmiao; Liu, Zheng; Zhang, Zaijun; contributed towards reference search, article writing, and proof reading.

## Address reprint requests to

Dr. Zaijun Zhang,

Institute of New Drug Research, Jinan University College of Pharmacy, Guangzhou 510632, China

Email: [zaijunzhang@163.com](mailto:zaijunzhang@163.com)

## Core tip:

Duchenne muscular dystrophy (DMD) is an X-linked inherited neuromuscular disorder due to mutations in the dystrophin gene. Animal models that accurately reflect pathological conditions and disease characteristics are key factors in the discovery and development of new anti-DMD drugs. Here, we described a novel DMD mouse model built up by the Nanjing Biomedical Research Institute of Nanjing University (NBRI). We found that the DMD mouse showed significant behavioral disorders and exhibited increased serum creatine kinase (CK) and lactate dehydrogenase. Western blotting and Immunofluorescence staining also showed significantly decreased expression level of dystrophin in the gastrocnemius (GAS) muscle. Besides, the mdx mouse of DMD developed fibrosis in both GAS and diaphragm (DIA). Taken together, our results indicated that the behavioral, biochemical and pathological characterization of the mdx mouse model is consistent with human DMD. This genetic mouse model may provide insights into the pathophysiology of DMD and the effects of anti-DMD drugs.

## Abstract:

**Background** Duchenne muscular dystrophy (DMD) is an X-linked inherited neuromuscular disorder due to mutations in the dystrophin gene. Animal models that accurately reflect pathological conditions and disease characteristics are key factors in the discovery and development of new anti-DMD drugs.

**Aim** Here, we evaluated motor behavior, pathological and biochemical characters of a new DMD mouse model built up by the Nanjing Biomedical Research Institute of Nanjing University (NBRI).

**Methods** The pole test and open-field test were used to assess the movement disorders in DMD mouse model. The gastrocnemius (GAS), biceps, triceps, soleus, and tibialis anterior muscles of mice were subjected to

weight analysis to evaluate the skeletal muscle pseudohypertrophy. Meanwhile, immunofluorescence and Western blotting were used to detect the expression of dystrophin in the GAS. Serum levels of creatine kinase (CK) and lactate dehydrogenase (LDH) that accurately reflect muscle damage were detected. Masson staining was used to evaluate the fibrosis of GAS and diaphragm (DIA).

**Results** The novel DMD mouse showed significant behavioral disorders and exhibited high serum levels of CK and LDH. Western blotting and immunofluorescence staining showed decreased significantly with dystrophin level in the GAS. Besides, the mdx mouse of DMD developed fibrosis in both GAS and DIA.

**Conclusion** Taken together, our results indicated that the behavioral, biochemical and pathological characterization of the mdx mouse model is similar to human DMD. This mdx mouse model may provide insights into the pathophysiology of DMD and the effects of anti-DMD drugs.

**Key words** Duchenne muscular dystrophy; Behavioral disorder; Creatine kinase; Dystrophin; Fibrosis

## INTRODUCTION

Duchenne muscular dystrophy (DMD) is an X-linked recessive genetic disease. Most clinical patients are male, while women are mainly pathogen carriers with mild symptoms <sup>1</sup>. DMD is primarily caused by mutations in the gene that encodes the dystrophin, resulting in loss of dystrophin function. Dystrophin functions as a cell scaffold to maintain muscle fiber integrity and muscle contraction. Usually, the clinical symptoms such as bradykinesia, abnormal gait, difficulty in standing, and the tendency toward falling appear at the aged of 3 to 5 in patients. Children with DMD older than 7 years old are usually unable to walk and require a wheelchair. After the age of 12, the disease progressively deteriorates <sup>2</sup> and most patients die around the age of 20 due to respiratory and circulatory failure <sup>3</sup>. Fibrosis is a prominent pathological feature in patients with DMD, which directly leads to muscle dysfunction <sup>4</sup>. Follow-up studies of 25 DMD patients with an average age over 10 showed that intramuscular fibrosis was uniquely associated with poor motor outcomes; the initial muscle biopsy showed pathological features such as muscle fiber atrophy, necrosis, and steatosis <sup>5</sup>. Respiratory failure is one of the leading causes of death in DMD patients <sup>6</sup>.

The animals used in DMD research are diverse, including mice, dogs, cats, fish, and *Caenorhabditis Elegans* <sup>7</sup>. Mice are used in the primary pre-clinical DMD research for the well-known physiological and genetic characteristics. The most commonly used mouse model strain is the C57BL/10ScSn-Dmd<sup>mdx</sup> model mouse <sup>8</sup>, which spontaneously mutated from normal British C57BL/10ScSn mice in 1977. A nonsense point mutation in exon 23 of dystrophin gene led to the early appearance of the stop codon, resulting in loss of expression of the full-length dystrophin <sup>8, 9</sup>. Mdx mice were found increased creatine kinase (CK) and pronounced muscle fibrosis. Yet, it exhibited a mild non-progressive phenotype. Because large-scale muscle fiber necrosis generally occurred at 20 days of age. Then, the muscle regeneration process was well compensated after 60 days and muscle fiber destruction is much lower after 120 days <sup>10</sup>.

Therefore, we commissioned Nanjing Biomedical Research Institute of Nanjing University (NBRI) to construct a novel DMD mice model through gene- edition in the *Dmd* exon 4 using the CRISPR/Cas9 and blastocyst injection technology. We assessed the new model from both the physical symptoms and the primary biomarkers (serum CK, LDH, muscle fibrosis, *et al.*) of DMD. This study may provide a new mouse model and methods for pre-clinical research of DMD therapy.

## MATERIALS AND METHODS

### ANIMALS

Seven-week-old male mouse (C57BL/10ScSnJNju-Dmd<sup>em3Cd4/Nju</sup>) and wild-type littermate controls were purchased from Nanjing Biomedical Research Institute of Nanjing University, China. The mice were housed at 23 ± 2 °C with a 12 h light/dark cycle and fed standard rodent chow and water *ad libitum*. The mice were acclimatized for one week before the experiments. All animal procedures were performed in accordance with the US NIH's "Guide for the Care and

Use of Laboratory Animals” and approved by the Animal Ethics Committee of the Guangzhou University of Chinese Medicine, China (Approved number # 20181104002).

### CRISPR/Cas9-MEDIATED MICE GENOME EDITION

KO mice were created using the CRISPR/Cas9 technique. gRNAs were designed based on the targeted sequences in the mouse *mdx* genes (Gene ID: 13405) and were generated by inserting gRNAs into pUC57 via BbsI restriction sites. The Cas9 gene (pSpCas9n(BB)-2A-Puro) was driven by a CMV promoter and the gRNA and its RNA scaffold by a T7 promoter. gRNA sequences are as follows: *mdx* exon 4 sgRNAs: 5'-TGCCTTGTTGACATTGTTCAggg-3', 5'-ACCGGAACAGTCTGCACACCagg-3', 5'-CTTG TAGATCCCTTTTCTTT tgg-3', 5'-CAATGTCAACAAGGCACTGCcgg-3'. Cas9 mRNA and sgRNAs were transcribed *in vitro*, and then were co-injected into the zygotes' pronuclei at a concentration of 2.5 ng/ $\mu$ L. After the injection, zygotes were left for 4-6 h before being introduced into pseudopregnant host females and carried to term. Edited founders were identified by Sanger sequencing from digit biopsies. Mice carrying the frameshift mutation were crossed with C57BL/10ScNJ to ensure germline transmission and eliminate any possible mosaicism. Heterozygous animals with the same modification were then mated to generate homozygous offspring.

### EXPERIMENTAL DESIGN

Experiments were procedure at 8 weeks. Behavioral tests were performed every 4 weeks. After 32 weeks, the mice were euthanized with 0.1% pentobarbital sodium (0.15 mL/10 g). Blood was drawn and the levels of ATP, CK, LDH, and superoxide dismutase (SOD) were measured. Immunofluorescence, Western blotting and Masson staining were also conducted in both DIA and GAS muscles.

### BEHAVIORAL TEST

The open-field test is an experimental test used to evaluate general locomotor activity levels. It was performed as previously described<sup>11</sup>. Mice were placed in the center of the apparatus (50 × 50 × 50 cm) with a division of nine equal rectangles on the ground. The 5 minutes total distance of motion trace of each mouse were analyzed. As previously described<sup>12</sup>, motor disorders in mice were also evaluated with a pole test using a homemade 50 cm stake with a diameter of 1 cm. The total time required for mouse to descend to the base of the pole is recorded for three trials.

### IMMUNOFLUORESCENCE STAINING

Immunofluorescence staining was performed as previously described<sup>11</sup>. Briefly, GAS muscle slides were incubated with the anti-dystrophin antibody (Abcam, ab15277) at 5  $\mu$ g/mL overnight at 4 °C. The slides were then washed with TBST and incubated with the rabbit anti-mouse Alexa Fluor 488 conjugate secondary antibody (FD bio science, FDR007) in the dark at room temperature for 1 hour. Then, the slides were washed in TBST and counter stained with 4, 6-diamino-2-phenyl indole (DAPI) for 5 minutes. Images of the slides were captured with an inverted fluorescence microscope (Olympus Corporation, Japan).

### WESTERN BLOTTING ANALYSIS

Protein samples were loaded onto 10% or 12% polyacrylamide gels, and then electroblotted onto poly (vinylidene fluoride) (PVDF) membranes. After the membrane was blocked with 5% skim milk at room temperature for 1.5 hours, the membrane was covered with the specific primary antibody overnight at 4 °C. The primary antibodies used in the study included anti- $\beta$ -actin (CST, 8457S), anti-dystrophin (Abcam, ab15277), and anti-TGF- $\beta$ 1 (Abcam, ab92486). After washed with TBST, membranes were incubated with the anti-mouse IgG-HRP conjugated secondary antibody (1:2000) for further 1.5 hours. The ECL kit (Ford Biology, FD8020) was used to detect the proteins bound that were analyzed with a digital imaging system (Carestream

Health, IS4000MMPro). The band intensities were quantified using the Carestream Molecular Imaging software.

### SERUM MEASUREMENT

Changes of enzyme levels in muscle disease, which are directly related to muscle fiber necrosis or muscle damage and reflect the underlying disease processes<sup>13</sup>. Serum CK and LDH are commonly used to help diagnose muscular dystrophy<sup>14, 15</sup>. The blood was clotted at room temperature for 30 minutes and then centrifuged at 1,500 r/minutes for 15 minutes to obtain the supernatants. The serum levels of CK, LDH, and SOD were measured using an automatic biochemical analyzer (Hitachi, Japan) according to the kit instructions (Xinyou Biotechnology, China). Values are reported as international units per liter (U/L).

### ATP CONTENT ASSAY

The ATP level in GAS was detected using an ATP assay kit (Beyotime, S0026)<sup>16</sup>. Briefly, 30 mg GAS was fully lysed by adding 300  $\mu$ L ATP lysis buffers for 30 minutes. The homogenate was centrifuged at 12,000 r/min for 15 minutes at 4 °C. According to the instructions, 50  $\mu$ L of the sample homogenate was added to 50  $\mu$ L ATP detection working solution and gently mixed. The OD value was measured at 570 nm using a multi-functional microplate reader (Bio Tek Corporation, USA). The ATP level in GAS was determined by a standard curve generated in the same assay.

### MASSON STAINING

Paraffin-embedded muscle tissue slides (4  $\mu$ m thick) in the DIA and GAS were deparaffinized in xylene, rehydrated in a graded alcohol series, and stained with Masson staining kit (Solarbio, G1340). The areas of fibrosis in DIA and GAS were measured using Materials Image Processing and Automated Reconstruction (MIPAR™) software (China)<sup>17</sup>.

### STATISTICAL ANALYSIS

All results were expressed as means  $\pm$  SEM. Data analyses were performed with GraphPad Prism software 6.0 (GraphPad, San Diego, CA, USA). An unpaired two-tailed Student's t test or two-way ANOVA, were used for comparison between groups. A difference was considered statistically significant at  $P < 0.05$ .

## RESULTS

### BEHAVIORAL DISORDERS IN DMD MODEL MICE

In the open-field test, the movement distance of the model mice was significantly decreased from the 12<sup>th</sup> week compared with the WT mice (**Fig. 1 A, B**). Moreover, the model mice spent more time climbing down from the pole than the WT mice (**Fig. 1 C**), which indicated that the coordination of model mice was significantly worse than that of WT. More importantly, the movement disorders of model mice still appeared at the end of the experiment, which meant that the dyskinesia derived from the gene modification was stabilized.

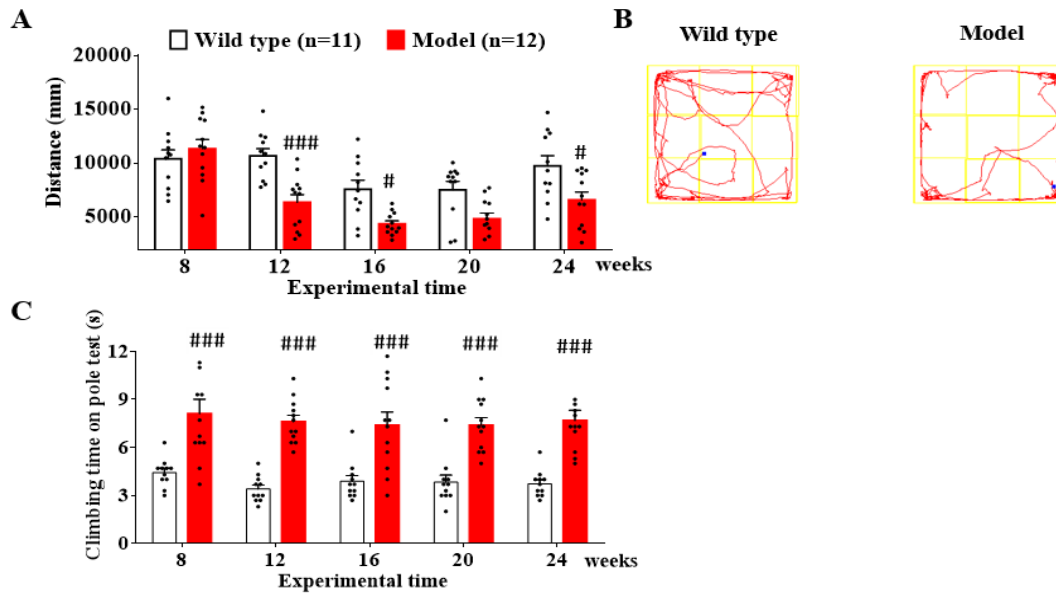


**Figure 1** Behavioral disorders in model mice. (A) Total distance travelled in the open-field test; (B) Trajectories of WT and model mice in the open-field test. (C) Climbing time on pole test. Data are represented as mean  $\pm$  SEM, # $P < 0.05$  and ### $P < 0.001$  relative to WT mice determined by two-way ANOVA.

### MUSCLE WEIGHT OF MODEL MICE

It has been reported that hypertrophy in DMD patients is caused by deposits of fat and connective tissue. The body weight gradually decreases in late adolescence<sup>18,19</sup>. However, the increased muscle weight in the mdx mouse presented similar incomprehensible feature of muscle hypertrophy as DMD patients<sup>19,20</sup>. Such conditions lead to an unstable posture and joint contraction. As we observed, the weight of soleus, biceps brachii, and triceps brachii in model mice significantly increased than those in the WT group (**Fig. 2 C, E, F**), while there was no noticeable difference in the GAS and tibialis anterior (**Fig. 2 B, D**).

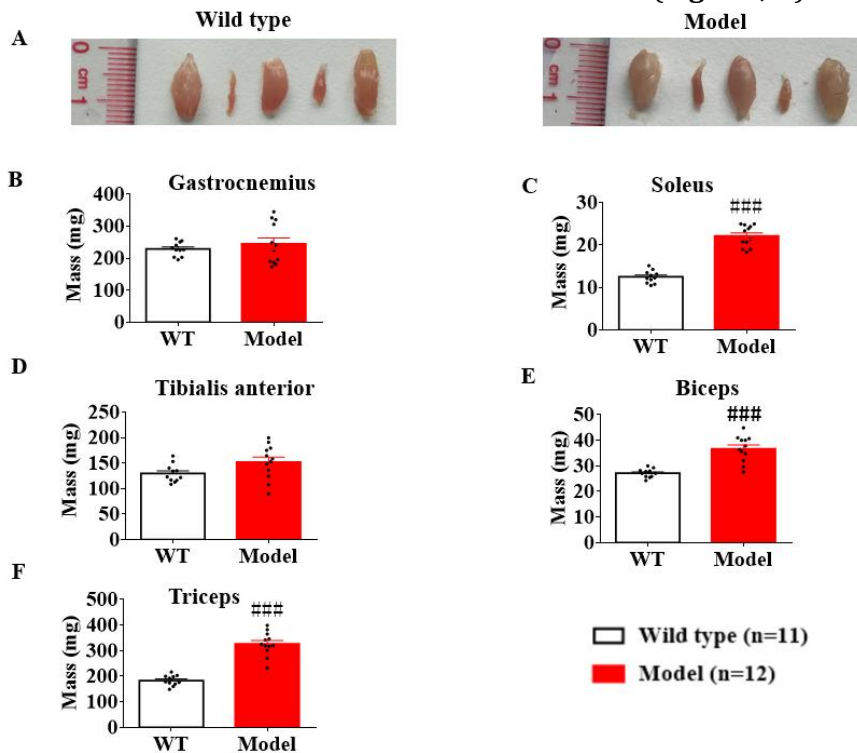


**Figure 2** Isolated muscle mass of model mice. (A) Isolated skeletal muscle; from left to right: gastrocnemius, soleus muscle, tibialis anterior muscle, biceps, and triceps; (B) - (F) Weight statistics of five isolated skeletal muscles. Data are represented as mean  $\pm$  SEM, ### $P < 0.001$  by t-test.



**DYSTROPHIN DEFECT IN DMD MODEL MICE**

Dystrophin is localized on the cytoplasmic surface of the sarcolemma and has a cell scaffold function to maintain muscle fiber integrity and muscle contraction<sup>21</sup>. Both immunofluorescence and Western blotting results of GAS showed similar significant reductions in the dystrophin expression in the model's skeletal muscles (**Fig. 3**). These results suggested that muscle fiber integrity and muscle contraction were somewhat disrupted.

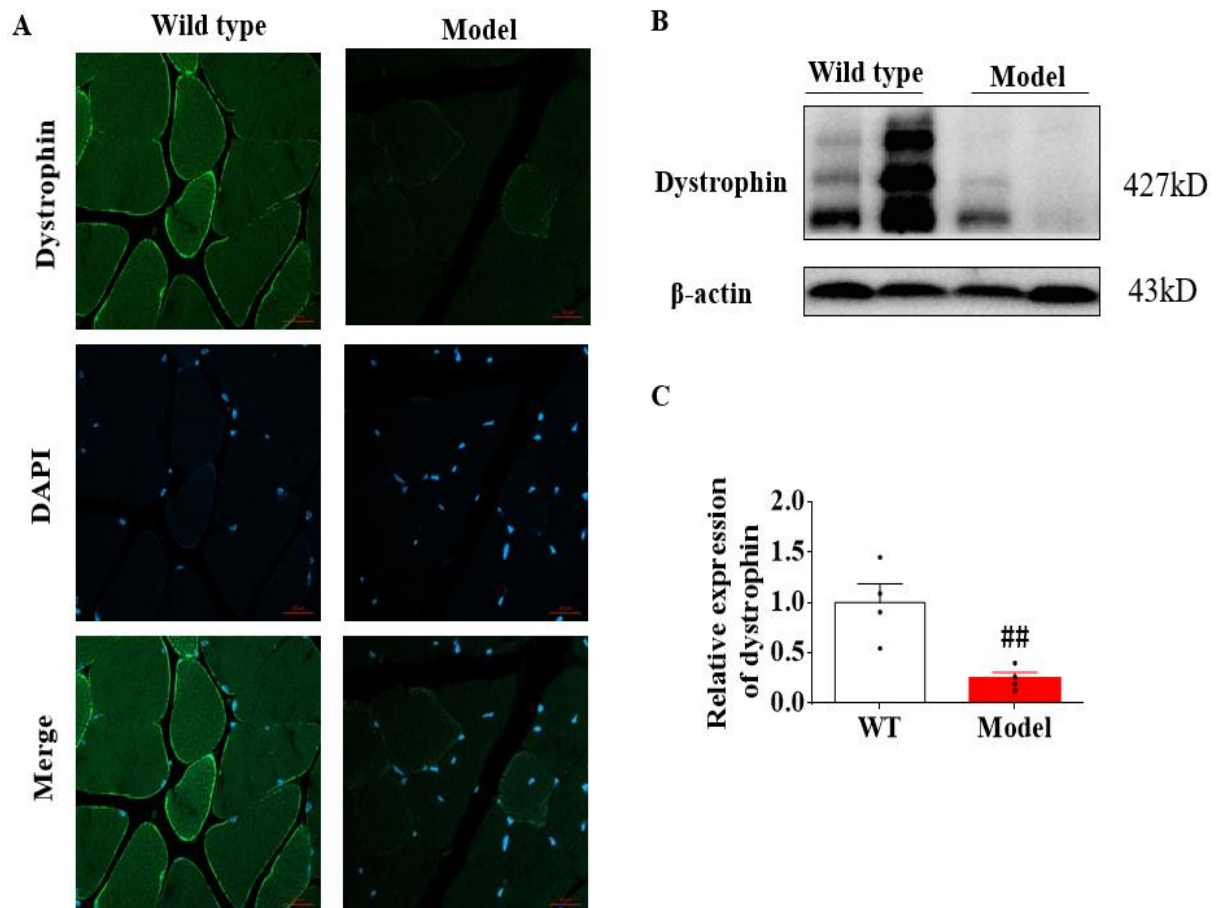


**Figure 3** Dystrophin is impaired in model mice. (A) Immunofluorescence staining of dystrophin in GAS (scale bar, 20 $\mu$ m). (B) Western blot analysis of dystrophin in GAS. (C) Quantification of the expression level of dystrophin in the mouse model and WT muscle. Data are represented as mean  $\pm$  SEM.  $##P < 0.01$  by t-test. Four mice/group. DAPI= 4,6-diamino-2-phenyl indole.

**SERUM CK AND LDH ELEVATED IN MODEL MICE**

Serum CK is a hallmark of clinical DMD diagnosis for reflection of muscle damage<sup>22</sup>. Serum CK level in DMD patients is usually high at a range of 5,000 to 150,000 U/L (while that in normal people is less than 200 U/L)<sup>23</sup>. Serum LDH levels also reflect tissue damage. The results showed that CK and LDH levels were significantly elevated in the model mice compared to the WT group (**Fig. 4 A, B**), indicating severe muscle and tissue damage in the model group.

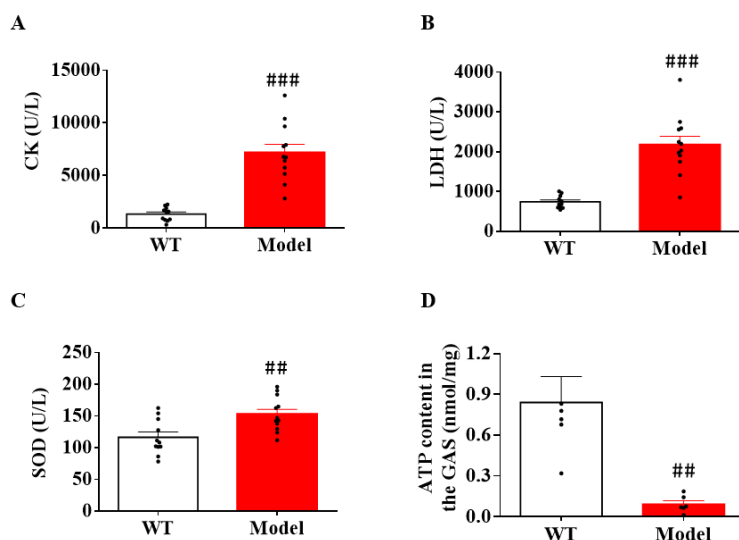


**Figure 4** Model mice show muscle damage and mitochondrial dysfunction. (A) Serum CK levels. (B) Serum LDH levels. (C) Serum SOD levels. (D) ATP level of the GAS. Data are represented as mean  $\pm$  SEM. # $P < 0.05$ , ## $P < 0.01$  and ### $P < 0.001$  by t-test. Six mice/group. CK= Creatine kinase; LDH= Lactate dehydrogenase; SOD= Superoxide dismutase.

### MODEL MICE HAVE MITOCHONDRIAL DYSFUNCTION

We detected serum SOD and ATP levels in GAS, which are associated with mitochondrial dysfunction. The experimental results showed that the serum SOD level of model mice was significantly higher compared to the WT. On the contrary, the ATP level dramatically decreased in the model group (**Fig. 4 C, D**). These data demonstrated that there may be mitochondrial damage in the DMD model mice.

### SEVERE MUSCLE FIBROSIS IN MODEL

Fibrosis is a pathological feature observed in DMD patients and *mdx* mice<sup>24, 25</sup>. To quantify the level of muscle fibrosis, we performed Masson staining on GAS and DIA, and then used MIPAR image analysis software to statistically analyze collagen. As illustrated in **Fig. 5 A-D**, masson staining showed that the fibrotic area of GAS and DIA in the model mice was much larger than that in the WT group, indicating severe fibrosis of GAS and DIA in model mice. The data showed in **Fig. 5C and E** demonstrated a significant up-regulation of TGF- $\beta$ 1 in GAS, which is in accordance with the published literature<sup>26</sup>.

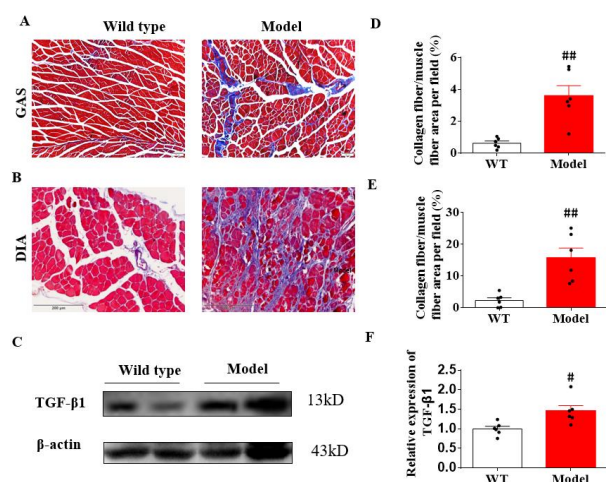


**Figure 5** Severe fibrosis of GAS and DIA in model mice. (A) Masson staining of the GAS, the cytoplasm, and muscle fibers are stained red while the collagen fibers appear blue (scale bar, 200 $\mu$ m). (B) Masson staining of the DIA (scale bar, 200 $\mu$ m). (C) Quantitative analysis of GAS muscle fibrosis. (D) Quantitative analysis of DIA muscle fibrosis. (E) Western blot analysis of TGF- $\beta$ 1 in the GAS. (F) Quantitative analysis of TGF- $\beta$ 1 in the GAS. Data are represented as mean  $\pm$  SEM. # $P < 0.05$  and ## $P < 0.01$  by t-test. Six mice/group. GAS= Gastrocnemius; DIA= Diaphragm.

## DISCUSSION

DMD is a rare disease. Usually, patients behave normally at birth, and gradually lose motor ability after seven years<sup>2</sup>. In one-third of patients, the lacking or insufficient of dystrophin which derived from the partial or points mutations in the stop codon of the dystrophin gene is the underlying mechanism of the disease<sup>27</sup>. Dystrophin deficiency in DMD leads to the instability of myocyte membranes and an uncontrolled influx of calcium. This triggers a series of pathological processes that eventually lead to protein break down and cell damage in muscle cells. Subsequently, muscle tissue is replaced by fibroblasts and fat cells, resulting in collagen deposits (fibrosis). Later, the pseudo-hypertrophy of the calf muscles and the gradual weakness of the proximal limb muscles inevitably lead to wheelchair dependence<sup>28</sup>.

A suitable animal model can reliably predict human responses to a given therapeutic intervention. Several DMD animal models, such as dogs, cats, mice, fish, and invertebrates have been constructed<sup>7, 29</sup>. Nevertheless, murine models are valuable for research because it is easy to breed and genetically engineer them compared to other large animal models. Though *mdx* mouse is the most widely used animal model for DMD, it shows a mild phenotype that differs from human. So, we are committed to designing a novel mouse model with a more severe phenotype.

CRISPR/Cas9 is a fast-growing genomic editing tool that is widely used in drug discovery and the development of animal models<sup>30, 31</sup>. NBRI targeted the gRNA of the mouse *Dmd* exon 4 using CRISPR/Cas9 and blastocyst injection technology. Then they screened for a mouse model that caused a frame shift mutation in the *Dmd* gene. And the model mouse is the background of C57BL/10, consistent with the *mdx* mouse model<sup>8</sup>.

The *mdx* shows no obvious muscle weakness that differs from human while DMD mice have behavioral disorders in the 8<sup>th</sup> weeks and last for 24 weeks. The creatine kinase level in *mdx* mice is significantly higher than that in normal mice; however, it gradually decreases in the fifth week and eventually reaches 4000-6000 U/L at the 23<sup>rd</sup> week<sup>32</sup>. Meanwhile, the creatine kinase levels in the model mice reach 6393-7973 U/L at 32 weeks, indicating that the muscle damage is more severe. Besides, the results showed that soleus, biceps, and triceps muscle in model mouse were obvious pseudo-hypertrophy and with increased mass. The immunofluorescence of dystrophin on the surface of the GAS membrane showed dimmer, which was consistent with the results of immunoblotting. And the model mice had lower ATP levels in the GAS. Besides, severe fibrosis was observed in the GAS and DIA muscles of model mice.

Of course, we need more experiments to determine the stability and reproducibility of the model and to perform further pathological analysis on other muscles, such as the myocardium<sup>33</sup>. More importantly, it is necessary to determine the onset time and pathological process of model mice to better assist in drug development.

## CONCLUSIONS

Currently, the establishment of an effective experimental model will help to screen a large number of drugs and make a significant contribution to drug advancement in the clinical arena. Our preliminary data on mouse model suggested that the model mice had a similar motor deficit and muscle pathology to human DMD. Thus, this mouse model may be a potential tool for exploring DMD drugs in the future.

## ACKNOWLEDGMENT

We thank Linda Wang for editing this manuscript.

## REFERENCES

1. Govoni A, Magri F, Brajkovic S, et al. Ongoing therapeutic trials and outcome measures for Duchenne muscular dystrophy. *Cell Mol Life Sci*. 2013;70(23):4585-4602. doi:10.1007/s00018-013-1396-z. [\[PubMed\]](#)
2. Jennekens FG, ten Kate LP, de Visser M, Wintzen AR. Diagnostic criteria for Duchenne and Becker muscular dystrophy and myotonic dystrophy. *Neuromuscul Disord*. 1991;1(6):389-391. doi:10.1016/0960-8966(91)90001-9. [\[PubMed\]](#)



3. Finsterer J. Cardiopulmonary support in duchenne muscular dystrophy. *Lung*. 2006 Jul-Aug;184(4):205-215. doi: 10.1007/s00408-005-2584-x. [\[PMc\]](#)
4. Mann CJ, Perdiguero E, Kharraz Y, et al. Aberrant repair and fibrosis development in skeletal muscle. *Skelet Muscle*. 2011;1(1):21. doi:10.1186/2044-5040-1-21. [\[PubMed\]](#)
5. Desguerre I, Mayer M, Leturcq F, Barbet JP, Gherardi RK, Christov C. Endomysial fibrosis in Duchenne muscular dystrophy: a marker of poor outcome associated with macrophage alternative activation. *J Neuropathol Exp Neurol*. 2009;68(7):762-773. doi:10.1097/NEN.0b013e3181aa31c2. [\[PubMed\]](#)
6. Melacini, P.; Vianello, A.; Villanova, C., et al. Cardiac and respiratory involvement in advanced stage Duchenne muscular dystrophy. *Neuromuscular Disorders*. 1996; 6: 367-376. doi:10.1016/0960-8966(96)00357-4. [\[PubMed\]](#)
7. McGreevy JW, Hakim CH, McIntosh MA, Duan D. Animal models of Duchenne muscular dystrophy: from basic mechanisms to gene therapy. *Dis Model Mech*. 2015;8(3):195-213. doi:10.1242/dmm.018424. [\[PubMed\]](#)
8. Bulfield G, Siller WG, Wight PA, Moore KJ. X chromosome-linked muscular dystrophy (mdx) in the mouse. *Proc Natl Acad Sci U S A*. 1984;81(4):1189-1192. doi:10.1073/pnas.81.4.1189. [\[PubMed\]](#)
9. Gillis, J. M. Understanding dystrophinopathies: an inventory of the structural and functional consequences of the absence of dystrophin in muscles of the mdx mouse. *Journal of Muscle Research & Cell Motility*. 1999; 20: 605-625. doi:10.1023/a:1005545325254. [\[PubMed\]](#)
10. Tanabe Y, Esaki K, Nomura T. Skeletal muscle pathology in X chromosome-linked muscular dystrophy (mdx) mouse. *Acta Neuropathol*. 1986;69(1-2):91-95. doi:10.1007/BF00687043. [\[PubMed\]](#)
11. Wu L, Su Z, Zha L, et al. Tetramethylpyrazine Nitron Reduces Oxidative Stress to Alleviate Cerebral Vasospasm in Experimental Subarachnoid Hemorrhage Models. *Neuromolecular Med*. 2019;21(3):262-274. doi:10.1007/s12017-019-08543-9. [\[PubMed\]](#)
12. Xu B, Zheng C, Chen X, et al. Dysregulation of Myosin Complex and Striated Muscle Contraction Pathway in the Brains of ALS-SOD1 Model Mice. *ACS Chem Neurosci*. 2019;10(5):2408-2417. doi:10.1021/acchemneuro.8b00704. [\[PubMed\]](#)
13. Gasper MC, Gilchrist JM. Creatine kinase: a review of its use in the diagnosis of muscle disease. *Med Health R I*. 2005;88(11):398-404. [\[PubMed\]](#)
14. Zhang Y, Huang JJ, Wang ZQ, Wang N, Wu ZY. Value of muscle enzyme measurement in evaluating different neuromuscular diseases. *Clinica Chimica Acta; International Journal of Clinical Chemistry*. 2012 Feb;413(3-4):520-524. doi: 10.1016/j.cca.2011.11.016. [\[PMc\]](#)
15. Ebashi S, Toyokura Y, Momoi H, Sugita H. High creatine phosphokinase activity of sera of progressive muscular dystrophy. *The Journal of Biochemistry*. 1959; 46:103-104. <https://doi.org/10.1093/jb/46.1.103>. [\[Article\]](#)
16. Fang WJ, Wang CJ, He Y, Zhou YL, Peng XD, Liu SK. Resveratrol alleviates diabetic cardiomyopathy in rats by improving mitochondrial function through PGC-1 $\alpha$  deacetylation. *Acta Pharmacol Sin*. 2018;39(1):59-73. doi:10.1038/aps.2017.50. [\[PubMed\]](#)
17. Sosa JM, Huber DE, Welk B, Fraser HL. Development and application of MIPAR™: a novel software package for two- and three-dimensional microstructural characterization. *Integr Mater Manuf Innov*. 2014; 3: 123-140. [\[Article\]](#)
18. Martigne L, Salleron J, Mayer M, et al. Natural evolution of weight status in Duchenne muscular dystrophy: a retrospective audit. *Br J Nutr*. 2011;105(10):1486-1491. doi:10.1017/S0007114510005180. [\[PubMed\]](#)
19. Kornegay JN, Childers MK, Bogan DJ, et al. The paradox of muscle hypertrophy in muscular dystrophy. *Phys Med Rehabil Clin N Am*. 2012;23(1):149-xii. doi:10.1016/j.pmr.2011.11.014. [\[PubMed\]](#)
20. Duddy W, Duguez S, Johnston H, et al. Muscular dystrophy in the mdx mouse is a severe myopathy compounded by hypotrophy, hypertrophy and hyperplasia. *Skelet Muscle*. 2015;5:16. Published 2015 May 1. doi:10.1186/s13395-015-0041-y. [\[PubMed\]](#)
21. Zubrzycka-Gaarn EE, Hutter OF, Karpata G, et al. Dystrophin is tightly associated with the sarcolemma of mammalian skeletal muscle fibers. *Exp Cell Res*. 1991;192(1):278-288. doi:10.1016/0014-4827(91)90187-y. [\[PubMed\]](#)
22. Zatz M, Rapaport D, Vainzof M, et al. Serum creatine-kinase (CK) and pyruvate-kinase (PK) activities in Duchenne (DMD) as compared with Becker (BMD) muscular dystrophy. *J Neurol Sci*. 1991;102(2):190-196. doi:10.1016/0022-510x(91)90068-i. [\[PubMed\]](#)
23. Verma S, Anziska Y, Cracco J. Review of Duchenne muscular dystrophy (DMD) for the pediatricians in the community. *Clin Pediatr (Phila)*. 2010;49(11):1011-1017. doi:10.1177/0009922810378738. [\[PubMed\]](#)

24. Taniguti AP, Pertille A, Matsumura CY, Santo Neto H, Marques MJ. Prevention of muscle fibrosis and myonecrosis in mdx mice by suramin, a TGF- $\beta$ 1 blocker. *Muscle & Nerve*. 2011; 43: 82-87. doi:10.1002/mus.21869. [\[Article\]](#) [\[PubMed\]](#)
25. Cabrera D, Gutiérrez J, Cabello-Verrugio C, et al. Andrographolide attenuates skeletal muscle dystrophy in mdx mice and increases efficiency of cell therapy by reducing fibrosis. *Skelet Muscle*. 2014;4:6. doi:10.1186/2044-5040-4-6. [\[PubMed\]](#)
26. Gosselin LE, Williams JE, Deering M, Brazeau D, Koury S, Martinez DA. Localization and early time course of TGF-beta 1 mRNA expression in dystrophic muscle. *Muscle Nerve*. 2004;30(5):645-653. doi:10.1002/mus.20150. [\[PubMed\]](#)
27. Hoffman EP, Brown RH Jr, Kunkel LM. Dystrophin: the protein product of the Duchenne muscular dystrophy locus. *Cell*. 1987;51(6):919-928. doi:10.1016/0092-8674(87)90579-4. [\[PubMed\]](#)
28. Kohler M, Clarenbach CF, Böni L, Brack T, Russi EW, Bloch KE. Quality of life, physical disability, and respiratory impairment in Duchenne muscular dystrophy. *Am J Respir Crit Care Med*. 2005;172(8):1032-1036. doi:10.1164/rccm.200503-322OC. [\[PubMed\]](#)
29. Collins CA, Morgan JE. Duchenne's muscular dystrophy: animal models used to investigate pathogenesis and develop therapeutic strategies. *Int J Exp Pathol*. 2003;84(4):165-172. doi:10.1046/j.1365-2613.2003.00354.x. [\[PubMed\]](#)
30. Ahmad G, Amiji M. Use of CRISPR/Cas9 gene-editing tools for developing models in drug discovery. *Drug Discov Today*. 2018;23(3):519-533. doi:10.1016/j.drudis.2018.01.014. [\[PubMed\]](#)
31. Shrock E, Güell M. CRISPR in Animals and Animal Models. *Progress in Molecular Biology and Translational Science*. 2017 ;152:95-114. DOI: 10.1016/bs.pmbts.2017.07.010. [\[PMC\]](#)
32. Glesby MJ, Rosenmann E, Nylén EG, Wrogemann K, Serum CK, calcium, magnesium, and oxidative phosphorylation in mdx mouse muscular dystrophy. *Muscle Nerve*. 1988;11(8):852-856. doi:10.1002/mus.880110809. [\[PubMed\]](#)
33. Spurney CF, Sali A, Guerron AD, et al. Losartan decreases cardiac muscle fibrosis and improves cardiac function in dystrophin-deficient mdx mice. *J Cardiovasc Pharmacol Ther*. 2011;16(1):87-95. doi:10.1177/1074248410381757. [\[PubMed\]](#)

---

**Article citation:**

Fengjiao Wang, Jing Wen, Baojian Guo, Liangmiao Wu, Zheng Liu, Zhang Zaijun. Behavioral, biochemical and pathological characterization of a new *Mdx* mouse model of duchenne muscular dystrophy. *J Pharm Biomed Sci*. 2020; 10 (06): 119-128. doi: 10.5281/zenodo.3930105. Available at <http://www.jpjpbs.info>

---

**Conflicts of Interest:** No conflict of interest.

**Disclaimer:** Any views expressed in this paper are those of the authors and do not reflect the official policy or position of the Department of Defense.

**Source of funding:** None